ELSEVIER

Environmental Modelling & Software 15 (2000) 387–402

Environmental Modelling & Software

www.elsevier.com/locate/envsoft

Water resources in the desertification-threatened Messara Valley of Crete: estimation of the annual water budget using a rainfall-runoff model

B. Croke [a,*], N. Cleridou [a], A. Kolovos [1,b], I. Vardavas [b], J. Papamastorakis [b]

[a] *Environment Research Laboratory, Foundation for Research and Technology-Hellas, Heraklion, Crete, Greece*
[b] *Department of Physics, University of Crete, and Environment Research Laboratory, Foundation for Research and Technology–Hellas, Heraklion, Crete, Greece*

Received 1 August 1999; accepted 22 February 2000

Abstract

A simple rainfall-runoff model (Vardavas, I.M., 1988. A simple water balance daily rainfall-runoff model with application to the tropical Magela Creek catchment. Ecol. Model 42, 245–264) developed and applied to the tropical wet–dry Magela catchment in the Northern Territory of Australia has been modified and applied to the Mediterranean wet–dry Messara Valley catchment of Crete. The Messara Valley constitutes the most important agricultural region of Crete and is threatened by desertification due to falling groundwater levels. The steep topography of the Messara Valley necessitated the introduction of a two-component sub-surface flow in the rainfall-runoff model, with the slow component representing deep sub-surface flow from the mountains forming the north and south boundaries of the catchment. The original model was also modified to include estimation of the groundwater level fluctuations, and recharge in order to look at possible future exploitation scenarios. While the model was designed for catchments with distinct wet–dry periods, it has been successfully applied to the River Pang catchment in the UK GRAPES (GRAPES, 2000. GRAPES Technical Report, European Commission, ENV4 CT95-0186, 250 pp, March 2000). The model indicates that the Valley's surface and groundwater resources are very sensitive to climatic variations, with a natural drop in groundwater levels of about 10 m and little surface runoff being possible during drought years. The 20 m drop in the groundwater level over the past 10 years is due to the increased irrigation pumping in conjunction with drought years. The model also indicates that the Valley might have gone through cycles of near zero groundwater net recharge every 3–4 years starting in 1982 (an El Nino year).

Keywords: Rainfall-runoff model; Water balance; Desertification; Groundwater

Software availability

Program title: creek
Developer: B. Croke and I. Vardavas
Contact Address: B. Croke, CRES, Australian National University, Canberra 0200, ACT, Australia
Year first available: 1999
Hardware required: PC
Program language: FORTRAN

1. Introduction

The over-exploitation of limited water resources in the Mediterranean region, in conjunction with possible future climatic change impacts, has led to a concern over their sustainability and the region's vulnerability to desertification (e.g., Fantechi et al., 1995). The island of Crete is located in the south eastern Mediterranean region of Europe and has a dry sub-humid climate, according to the definitions of the June 1994 Paris Convention on Desertification (UNCED, 1994). It is a region that is designated susceptible to land degradation arising both from climatic variation and land-use activities. Part of the Earth Summit (UNCED, 1992) was concerned with the worldwide effort to curb land degradation by

* Address for correspondence: B. Croke, CRES, The Australian National University, Integrated Catchment Assessment and Management Centre, Bldg 43, Canberra ACT 0200, Australia.
E-mail address: bfc@cres.anu.edu.au (B. Croke).
[1] Now at Department of Environmental Sciences and Engineering, The University of North Carolina at Chapel Hill.

1364-8152/00/$ - see front matter
PII: S1364-8152(00)00018-9

combating desertification. In this context, there has been an effort in Crete to understand the role of climatic variation and land-use practices on the water resources of the island by focussing on groundwater resource overexploitation in its largest and most important catchment, that of the Messara Valley.

The Messara Valley covers an area of 398 km^2 and is located in the central-southern part of Crete, about 50 km south of the city of Heraklion (Fig. 1). The Valley constitutes the most important agricultural region of Crete. It is also the site for the Minoan palace of Phaistos and the Roman city of Gortys. About 250 km^2 of the total Valley area of 398 km^2 are cultivated. The main land-use activities are olive growing (about 175 km^2) and grape vine cultivation (40 km^2). The remainder of the cultivated land is used for vegetable, fruit and cereal growing. The Messara Valley has remained rural with a small population of about 40 000 inhabitants. The main source of irrigation water is groundwater as there is little surface water flow outside the winter months.

Groundwater is the key resource controlling the economic development of the region, it is also a component of the environment under siege as water demand has increased dramatically in the last ten years. The groundwater level is thus an important index for assessing both anthropogenic and climatic causes of desertification in the Valley.

Following the detailed agricultural development study conducted by the UN Food and Agriculture Organisation in 1972 (FAO, 1972) for the exploitation of the Valley's water resources, an extensive network of pumping stations has been installed since 1984 which has converted what used to be dry cultivation of olive trees to drip-irrigated cultivation. The consequences have been a rise in productivity and a dramatic drop of 20 m in the groundwater level. It is important to note that during the 1992–93 hydrological year (September to August) there was no river flow out of the Valley. This was the first time that the main river bed remained dry according to the records. The Valley's water resources have been monitored extensively for over twenty years by the Department of Agriculture in Crete. There are daily

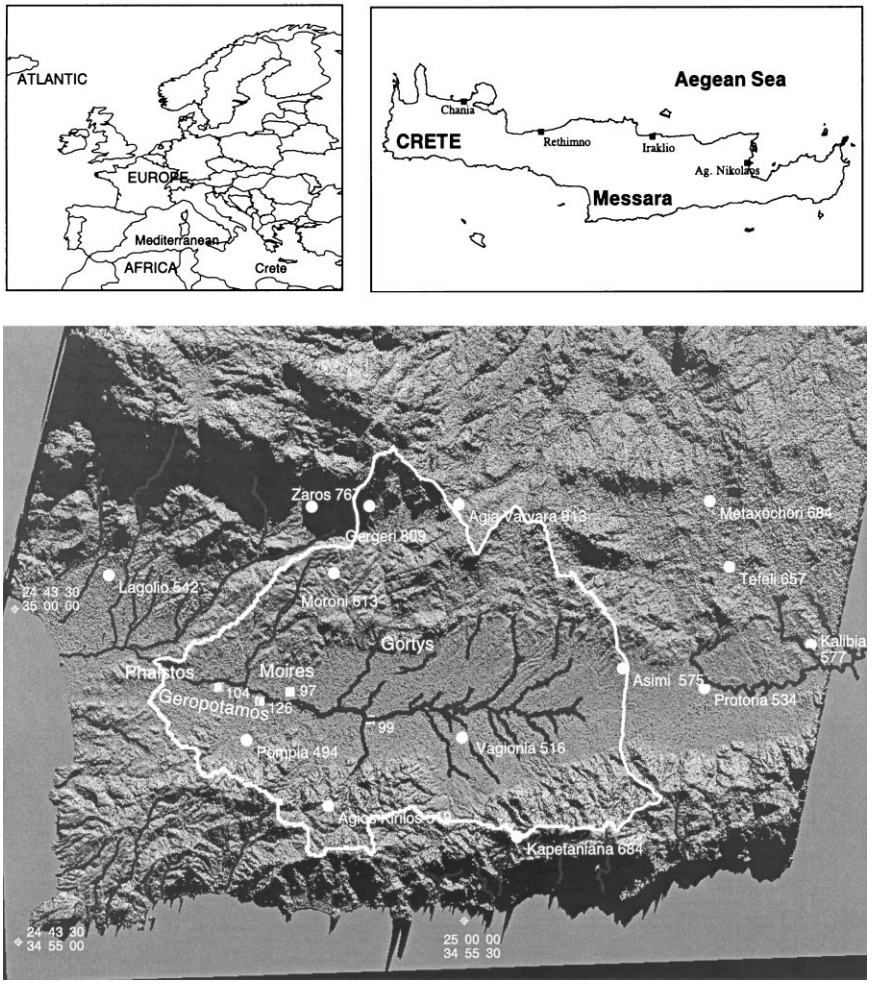

Fig. 1. The Messara Valley of Crete. Shown are the sites of the rainfall gauge stations, with mean annual precipitation following the name of each site. The Valley's river outlet is at the Phaistos constriction in the west, beyond which is the small coastal Timbaki Plain. Bore holes 97, 99, 104 and 126 are shown near the Geropotamos river. (Vardavas et al., 1996, by permission Department of Geography, University of Cambridge).

measurements of rainfall from 15 stations, daily measurements of runoff at the Valley's outlet at Phaistos, daily pan evaporation from 5 sites and monthly records of groundwater levels for over 25 sites.

Understanding the processes which control the seasonal water budget of the dry sub-humid Messara Valley is an important prerequisite for understanding groundwater level changes and the desertification processes in the Valley. Measurements and models of surface radiation fluxes, evapotranspiration, rainfall-runoff and groundwater levels are needed to determine the seasonal hydrological budget of the Valley and for relating it to land-use practices, and to atmospheric conditions, and hence to climatic variations.

The current study of the Messara Valley has been undertaken as part of the European Commission funded project GRAPES: Groundwater and River Resources Action Programme on a European Scale (GRAPES 1997, 1998), contract ENV4–CT95–0186. This project involves database collation and analysis of historical data for three catchments (River Pang in UK, Upper Guadiana in Spain and the Messara Valley in Greece), hydrological and hydrogeological modelling of the catchments, catchment management planning and expansion of findings to a Pan-European scale. The final goal is the production of guidelines providing strategies for sustainable water resources management.

Here, an improved rainfall-runoff model is presented and applied to the Messara Valley. The model is used to understand the partitioning of rainfall into the various surface and sub-surface stores and to determine the bulk daily water budget of the Valley, during the past twenty years and under future climatic conditions and land-use practices. To this end, we have modified the MAGELA rainfall-runoff model that was developed for the tropical wet–dry Magela catchment of the Northern Territory of Australia (Vardavas, 1988). The Mediterranean climate of Crete also exhibits distinct wet and dry seasons but the two catchments differ strongly in their topography.

The Magela Creek, which drains an area of approximately 600 km^2 within the Kakadu National Park in the Northern Territory of Australia, is relatively flat, and the creek flows only during the wet season. In comparison, the Messara Valley is defined by mountain ranges to the north and south which reach an elevation of more than 1 km above the Plain of the valley. In addition, the outlet of the catchment is narrow, confined to a channel cut into an impermeable barrier of lower Tertiary near Phaistos. As a result, there is stronger sub-surface flow, which is directed towards the catchment outlet. This results in a more significant base flow contribution to the surface discharge. In its natural state, the Geropotamos River of the Messara Valley flowed continuously, and there was a wetland located near the catchment outlet. The drop in the groundwater level has resulted in the wetland drying up, with no flow in the river in the dry season through the 1990s, and even in the wet season of 1992.

The MAGELA model was modified to account for the sub-surface flow from the mountains by including a two-component sub-surface flow comprising near surface flow to channels on the Plain (fast component) and deeper flow from the mountains (slow component). Other modifications include the introduction of a cutoff in the groundwater storage below which there is no contribution to the surface discharge from the groundwater store, or the deep sub-surface flow; and allowing for a natural loss mechanism for the groundwater store, accounting for both sub-surface outflow and evaporation of surface expressed groundwater. In addition, a technique to derive the daily runoff coefficient curve has been developed using Fourier deconvolution of the measured rainfall and discharge, used as part of the validation of the model.

The new version MESSARA model was validated with twenty years of daily rainfall and catchment discharge data. The model also gives an estimate of the seasonal variation of the mean unsaturated zone water content, the actual evapotranspiration loses and the mean groundwater level fluctuations. The model indicates that the groundwater store of the Messara Valley has a significant natural loss, through evaporation and sub-surface outflow to the sea. Mechanisms for possible evaporative loss of groundwater include evaporation from wetlands, and evapotranspiration in areas where the groundwater reaches the root zone (Llamas, 1988). Sub-surface groundwater flow to the sea is a common loss mechanism in coastal areas, especially where there are karstic limestone formations (Stringfield and LeGrand, 1971) as in Crete. This makes the Valley's water resources more susceptible to droughts, as demonstrated by the natural drop in the groundwater level by about 10 m in the early seventies, a period of well below average rainfall and little agricultural pumping.

The model also indicates that groundwater levels will not recover from their present 20 m drop for at least ten years with average rainfall (588 mm) and pre-irrigation network pumping rates. Further, by applying a GCM scenario for significantly reduced rainfall (annual mean reduced to 435 mm) by 2050, the model predicts a further drop of about 10 m if we have the average rainfall of a future drier climate and the present groundwater pumping rate. The model also indicates that there might be a 3–4 year cycle of near zero groundwater net recharge.

2. The Messara Valley

2.1. Relief and geology

The West Messara Valley catchment covers an area of 398 km^2 comprising an east–west Plain of 112 km^2

which is about 25 km long and about 3 km wide with steeply rising mountains on the north and south sides. To the north, the divide varies from 1700 m to 600 m from west to east, with the highest point being part of the Ida mountain range (peak at 2540 m) which is a limestone massif. To the south is the Asterousia mountain chain which rises 600 m in the west to 1200 m in the east and constitutes the southern most mountain range of Europe. At the Phaistos constriction in the west, the catchment outlet of the Geropotamos river is at 30 m above sea level (ASL). The catchment area of the northern slopes is 160 km^2 while the southern slopes constitute a catchment area of 126 km^2.

The Plain is covered mainly by Quarternary alluvial clays, silts, sands and gravels with thickness from a few metres to 100 m or more. The inhomogeneity of the Plain deposits give rise to great variations in the hydrogeologic conditions even over small distances. The northern slopes are mainly silty-marly Neogene formations while the southern slopes are mainly schists and limestone Mesozoic formations.

2.2. Water resources

The Messara hydrological year may be divided into a wet and dry season. About 40% of precipitation occurs in the months of December and January while from June to August there is negligible rainfall. Although the Valley receives on average (long-term) about 600 mm of rainfall per year it is estimated that about 65% is lost to evapotranspiration, 10% as runoff to sea and only 25% goes to recharging the groundwater store. Rainfall increases with elevation from about 500 mm on the Plain to about 800 mm on the Valley slopes while on the Ida massif the annual precipitation is about 2000 mm and on the Asterousian mountains it is 1100 mm. Pan evaporation is estimated at 1500±300 mm per year while the winds are mainly westerly. The potential evaporation is estimated at 1300 mm per year (Vardavas et al., 1997) and so the ratio of mean annual rainfall to potential evaporation for the Valley is about 0.5 and hence it is classified as dry sub-humid according to UNCED (1994) definitions. The average winter temperature is 12°C while for summer it is 28°C. Relative humidity in winter is about 70% while in summer it is about 60%.

The Plain contains several aquifers and aquicludes of complex distribution and properties. Groundwater levels are maximum in March or April with long recessions until recharge occurs in winter. The aquifers were high yielding with discharge rates as high as 300 m^3/hr in the early seventies but now are reduced to about one tenth of this. From pumping tests, the specific yield ranges between 0.05 and 0.15 while the horizontal transmissivity ranges between 0.1 and 0.01 m^2/s. Lateral groundwater outflow from the Valley is small compared with the vertical groundwater outflow. Before the installation of the groundwater irrigation system, the average discharge out of the Valley was about 20 Mm^3/yr corresponding to 50 mm of the annual rainfall lost as runoff to the sea.

3. Daily rainfall-runoff model

3.1. Model structure

The conceptual rainfall-runoff model (Vardavas, 1988) partitions daily rainfall into various stores, shown in Fig. 2, consisting of a vegetative cover interception store, a surface store, a soil store and groundwater store to predict the daily discharge from the catchment. The capacity of each store is L_m, D_m, S_m and G_m, respectively; and the storage given by L, D, S and G, respectively. The model consists of three phases: wetting, infiltration-runoff and drying phase, with modifications made to the infiltration-runoff phase. In the wetting phase, the daily precipition, P, is added to the interception store. If the total amount exceeds the capacity of the interception store, the excess (U) is passed to the surface store. The infiltration-runoff phase handles the movement of water to the soil and groundwater stores, and the production of the surface discharge. Details of this phase are given later. During the the drying phase water is taken to evaporate (E) first from the vegetative cover, then from the

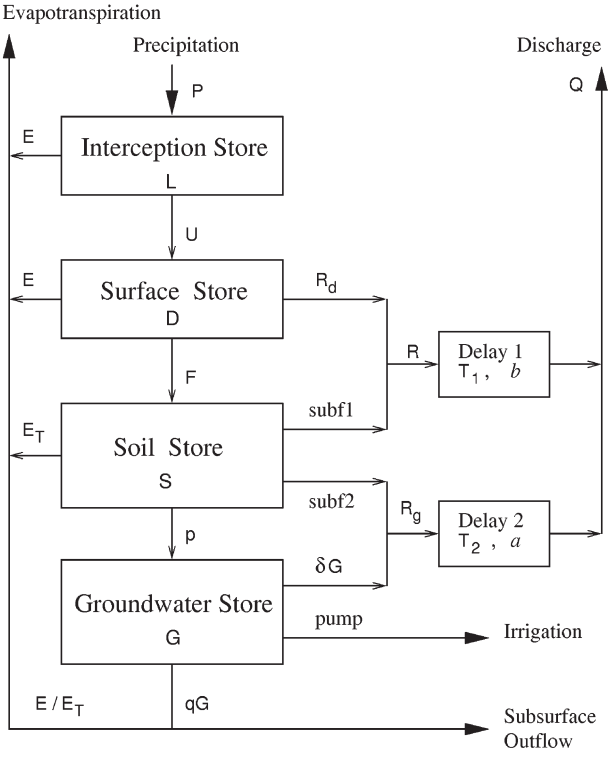

Fig. 2. Flow diagramme of the MESSARA conceptual rainfall-runoff model.

land surface and finally from evapotranspirate (E_T) from the soil store. Originally, for the Magela Creek catchment, evaporative losses from the groundwater store were included in the model. For the Messara Valley catchment, this process is included in the more general loss of water from the groundwater store given by q which also includes sub-surface outflow from the catchment.

The modified model has been validated for the Messara Valley catchment by its ability to predict the daily flow out of the catchment using the existing hydrological data record. The validated rainfall-runoff model provides an insight into the processes which govern the surface runoff and water budget of the Valley. The model is used to examine the hydrological response of the Valley to climatic variations, changing global climatic conditions according to a GCM scenario, and agricultural productivity through the linking of changes in rainfall-runoff processes to corresponding changes in groundwater levels.

3.2. Input data

Daily rainfall (mm) data are available from 13 stations at various locations on the Valley (Fig. 1). The daily rainfall and catchment discharge records cover all years from 1970. The mean catchment daily rainfall P is taken to be the weighted arithmetic mean value of the corresponding daily recordings made by the rainfall stations. The weight applied to each station was determined from the elevation of the station, and the density distribution of elevation in the catchment. As noted earlier, there is a variation in the measured rainfall with elevation. Fig. 3 shows the total rainfall for 1970 for the 13 stations, plotted against their elevation. The south side of the catchment clearly has a lesser dependence of rainfall with elevation compared with the north side. For the north and south side, the rainfall shows a linear trend with elevation, with the fits being, respectively:

$$P_i = 361 + 0.94 z_i \quad (1)$$

$$P_i = 470 + 0.19 z_i \quad (2)$$

where P_i and z_i are the rainfall (mm) and elevation (m) of a particular location in the catchment. The correlation coefficient R of these fits is 0.89 and 0.88, respectively. A digital terrain model (DTM) for the catchment was used to convert these equations into weights for each of the 13 rainfall stations. The weights for the stations were set to the number of pixels in the DTM with elevation values within the range of each station. The limits of the range in elevation for each station was taken to be the midpoint of the elevation of the station with that of the next highest and lowest station. In the case of the highest (and lowest) stations, the upper (and lower) limit was taken to be the catchment boundary in elevation.

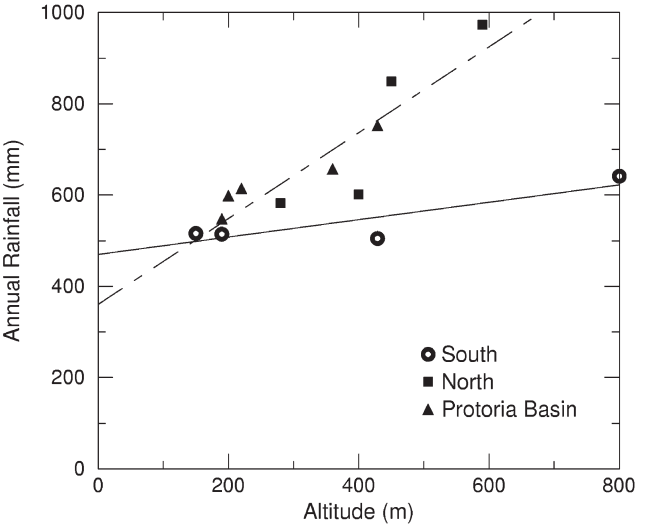

Fig. 3. Rainfall for each of the 13 stations plotted against elevation. Data from three regions are shown: north and south of the catchment, and in the neighbouring Protoria Basin (which closely matches the distribution for the north of the catchment). Also shown are the linear regressions for the south of the catchment (solid line) and the combination of the north of the catchment and the Protoria Basin (broken line).

A reasonable estimate under wet conditions is to set evaporation equal to potential evaporation (Brutsaert, 1984). Potential evaporation, E_p, was estimated from the data of five pan evaporation stations and using monthly mean lake-to-pan coefficients estimated from the potential evaporation via the Penman (1948) equation which requires meteorological and surface radiation budget data. A comparison between the monthly mean Penman evaporation and the mean pan evaporation data that are available for the catchment gives an estimate of the monthly variation of the pan coefficient. The potential evaporation for a specific year during the wet season is then given by

$$E_p = p_c \cdot E_{pan} \quad (3)$$

where E_{pan} is the measured pan evaporation and p_c is the pan coefficient whose variation in the Messara Valley is shown in Fig. 4 (Vardavas et al., 1997).

3.3. Modifications to the MAGELA model

The MESSARA model is a modified version of the original MAGELA model developed for the wet–dry tropical Magela Creek catchment in northern Australia (Vardavas, 1988). For the Magela Creek, the flow consists of a series of flood events superimposed on a base flow which stops before the end of the Wet season. In comparison, the natural state of the Messara Valley is for year round flow at the catchment outlet, with the base flow extending throughout the dry season. The first recorded period of no flow at Phaistos was in August

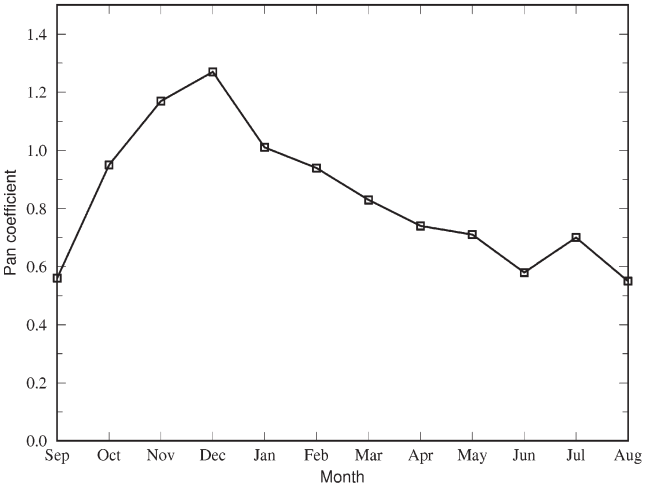

Fig. 4. Monthly mean pan coefficient.

1990. Since then, there has been no flow in the Dry season. Since mid 1992, there has been no evidence of the slow component in the measured discharge curve, with no flow recorded from June 1992 to November 1993. This coincides with the decrease in the groundwater level from the mid 1980s.

Modifications were made to the infiltration-runoff phase of the model, the excess surface water infiltrates into the soil store S up to the maximum infiltration rate for that day F given by:

$$F=F_0\cdot e^{-kS} \tag{4}$$

where $k>0$. If the excess surface water exceeds F, the remainder goes to local surface runoff R_d. The minimum infiltration rate F_c occurs when $S=S_m$. Under saturated soil conditions, the percolation rate, p, to the groundwater store is maximum given that the groundwater store is empty, thus

$$p=p_0\cdot\left(1-\frac{G}{G_m}\right)\cdot\frac{S}{S_m} \tag{5}$$

where G_m is the groundwater store capacity.

Next we consider lateral flow from the soil store. The original model required modification to include a two-component lateral sub-surface flow, *subf*1 representing relatively fast flow to the outlet (near-surface flow to channels on the Plain) and *subf*2 slower flow to the outlet (deeper flow from the surrounding hilly parts of the catchment), as shown in Fig. 2. The two components are given by:

$$subf1=\alpha F\left(\frac{S}{S_m}\right)^{\gamma} \tag{6}$$

and

$$suf2=\beta F\left(\frac{S}{S_m}\right)^{\gamma} \tag{7}$$

where α and β are the fractions of the daily infiltration F that contribute to each component, S is the amount of water in the soil store, S_m is the capacity of the soil store, and γ determines the sensitivity of the sub-surface flow on the fractional soil storage (S/S_m). Note that $0\leq\alpha+\beta<1$, since some of the infiltration will go to percolation.

The two-component sub-surface flow model allows for a delay between local runoff and discharge at the outlet of the order of days (fast component) and of the order of weeks (slow component). Without the introduction of the two-component sub-surface flow, the model is unable to reproduce both the peaks in the measured hydrograph, and the slow decrease in flow towards the end of the hydrological year. Optimising the model with β set to zero results in the delay parameter a for the fast flow store decreasing to nearly the same value as obtained for the delay parameter b for the slow store when the full model is used. This is a result of the large number of days affected by the slow flow component compared with the fast flow component. Thus the model discharge curve does not reproduce the observed flow peaks.

For the minimum value F_c we have

$$F_c=subf1_c+subf2_c+p_c \tag{8}$$

with

$$subf1_c=\alpha F_c \tag{9}$$

$$subf2_c=\beta F_c \tag{10}$$

and

$$p_c=p_0(1-G/G_{max}) \tag{11}$$

so that

$$F_c=\frac{p_c}{1-(\alpha+\beta)} \tag{12}$$

and we calculate the unknown parameter k in Eq. (7) from

$$k=-\frac{\ln(F_c/F_0)}{S_m} \tag{13}$$

The equation that describes the variation of S with time can be written as

$$\frac{dS}{dt}=W-subf1-subf2-p=A \tag{14}$$

where

$$W=\begin{cases}V & \text{, if } V\leq F\\ F(S) & \text{, if } F<V\end{cases} \tag{15}$$

We use the Euler–Trapezoidal integration method to

integrate Eq. (17) over a day. Thus, for the *i*th day and for time interval $\Delta t = 1$ day

$$S_i = S_{i-1} + \Delta t(A_i + A_{i-1})/2 \quad (16)$$

In the same way we can find the rate of change B of the groundwater storage G. Here, two modifications to the model were needed. First, a critical value G_0 in the groundwater storage was introduced, below which there is no contribution to the surface runoff from the groundwater store. This enables the discharge predicted by the model to become zero after August 1990, the first occasion when no flow was recorded at the Phaistos gauging station. When the groundwater storage falls below the critical value, the deep slow-flow component from the soil store stops. This is represented in the model by setting the value of β to zero when $G < G_0$. Physically, this is the result of the slow-flow component remaining a sub-surface flow when the base flow has ceased.

The second modification to the model concerning the groundwater store was the inclusion of a natural loss component q. This parameter allows for evaporative loss from the groundwater store, as well as sub-surface flow out of the catchment. Such flow is important in island catchments with karstic limestone formations such as the Messara Valley. The mean elevation of the Messara Plain is approximately 70 m above sea level, with the groundwater level about 20 m below the surface. The distance from the middle of the Plain to the sea is approximately 10 km to the south (beyond the Asterousian mountains) and to the west, through the south of the Timbaki basin. Thus there is a significant gradient in the watertable in an active geological region (Crete lies on the African continental plate, near the junction with the European plate). Thus B is given by:

$$\frac{dG}{dt} = p - \delta(G - G_0) + qG - pump = B \quad (17)$$

The equations are solved for the *i*th day using the Newton–Raphson method. We can then calculate the near-surface local flow R and deep sub-surface local flow R_g from

$$R = R_d + subf1 \quad (18)$$

$$R_g = subf2 + \delta G \quad (19)$$

Both R and R_g are accumulated via two delay stores T_1 and T_2, respectively, before reaching the catchment outlet. The discharge from each contributes to the total discharge at the outlet, Q, of the Valley

$$Q_{\mu,i} = k_\mu T_{\mu,i},\ \mu = 1,2 \quad (20)$$

where the coefficients $k_1 = b$, $k_2 = a$, are model parameters which determine the delay storages

$$T_{1,i} = (1-b)T_{1,i-1} + R \quad (21)$$

$$T_{2,i} = (1-a)T_{2,i-1} + R_g \quad (22)$$

Thus, the equation pair becomes

$$Q_{1,i} = bT_{1,i} \quad (23)$$

$$Q_{2,i} = aT_{2,i} \quad (24)$$

where $0 \le a < b$ and $a < b \le 1$. The parameters a and b will depend generally on the specific topographic and soil characteristics of the catchment. The closer to unity their value is the faster the local flow reaches the outlet.

The model's predictive capability was also increased by converting the model groundwater storage to a mean groundwater level for the aquifer. This was achieved by using measured values of the specific yield to estimate the mean effective porosity for the aquifer. This enables the model to be used to investigate the climatic and anthropogenic effects on the groundwater level, thus enabling prediction of future groundwater resources vital to agricultural areas in arid and semi-arid catchments. The model was also used to estimate the net recharge to the aquifer by comparing the annual rainfall with the total water lost from the catchment.

4. Model parameter selection

The model makes use of fourteen parameters to predict the discharge at the catchment outlet. For most of the parameters, selection is conducted so that the differences between model discharge Q_m and measured discharge Q_0 at the outlet is minimized. In order to achieve this we use as the objective function (e.g. Vardavas, 1989) χ^2, as defined by

$$\chi^2 = \frac{1}{N_d} \cdot \sum_i \chi_i^2 \quad (25)$$

where for the *i*th day

$$\chi_i^2 = \frac{(Q_{0_i} - Q_{m_i})^2}{Q_{0_i}} \quad (26)$$

and $_d$ are the degrees of freedom in the model

$$N_d = N - n_p - 1 \quad (27)$$

where N is the number of daily measurements and n_p is the number of model parameters. Note that for days when Q_{0_i} was zero, the denominator was set equal to 0.001 in order to calculate χ^2 for the 1990s. For a good match between the system behaviour and the model output it is required that $\chi^2 < 1$. We used an iterative Fibbonacci search technique (Vardavas, 1989) to minimize the objective function. The search technique for model parameter selection includes an automatic increase in the

search range if the optimum value of a given parameter lies outside the range chosen initially. Two parameters, G_0 and q, were determined from specific hydrological conditions. The value of G_0 was set to the groundwater store G at the end of the 1989/90 hydrological year, the first year to have zero flow out of the catchment. The value of q was determined from the drop in groundwater level in the early 1970s.

The parameters used in this model and their significance are shown in Table 1. The optimised parameter set was constrained within a range of values based on field measurement considerations as was done in Vardavas (1988). The inhomogeneity of the geological deposits of the Messara Plain is expected to give rise to great variations in the hydrogeologic conditions even over small distances. Nevertheless, to obtain a plausible range of values for the model parameters, especially those of the store capacities, we took representative values for the various catchment characteristics that determine our parameters. The range of interception and surface store capacities, maximum infiltration rate and maximum percolation rate from the soil to the aquifer were chosen along similar lines as in Vardavas (1988). The range of the soil store capacity was determined by adopting a soil depth of 1–2 m with a porosity of 25% for essentially alluvial silty-sandy soil, to obtain a range of 250–500 mm for S_m. For the groundwater store, we take an unconfined aquifer on the Plain with a typical depth between 30–100 m and an effective porosity of about 10% for a typical clayey-silty composition (de Rider, 1972) and based on pumping tests performed on the Messara Plain, to obtain a search range 1000–3000 mm for the groundwater store capacity G_m. The model was initially tested against daily data for the three hydrological years 1981–82, 1982–83 and 1983–84. These comprise two years which preceded the installation of the groundwater pumping network for irrigation.

The optimised set of model runoff parameters, and the sensitivity of the objective function, s, to each as defined by

$$s=\frac{\Delta\chi^2/\chi^2}{\Delta p/p} \tag{28}$$

are given in Table 2, for a 10% change in p. Also given are the values for the model parameters G_0 and q.

5. Model validation

Validation of the model was performed using four tests. These were:

1. 1. Value of the objective function (χ^2) of the differences between the model and measured discharge at the outlet for all years.
2. Comparison of the flow duration curves (standard technique for comparing the frequency distribution of the discharge) derived from the model output and the actual discharge data.
3. Comparison of the daily runoff coefficient (derived from Fourier analysis of the model and measured discharge data, together with the rainfall data) which gives the mean temporal response of discharge to a day's rainfall.
4. Comparison of model and measured groundwater level fluctuations derived from the groundwater storage based on a mean effective porosity for the aquifer.

The last two tests were developed in the present work.

Table 1
The set of model parameters

Parameter	Description
L_m	Interception store capacity
D_m	Surface store capacity
S_m	Soil store capacity
G_m	Groundwater store capacity
α	Fraction of S that goes to fast runoff
β	Fraction of S that goes to slow runoff
δ	Fraction of G that goes to runoff
F_0	Maximum infiltration rate
p_0	Maximum percolation rate
a	Delay coefficient for slow runoff
b	Delay coefficient for fast runoff
γ	Power law for contribution to surfaceflow from soil store
G_0	Minimum groundwater storage forcontribution to runoff
q	Fraction of groundwater storage lostthrough evaporation andsub-surface outflow

Table 2
Model parameter values and sensitivity of the objective function to 10% variation in parameter value. The search range is also shown

Parameter	Range	Value	Sensitivity
L_m (mm)	10–30	22.98	0.050
D_m (mm)	2–15	4.59	0.010
S_m (mm)	250–500	317.6	0.346
G_m (mm)	1000–3000	1516.9	0.043
α	0–1[a]	0.380	0.121
β	0–1[a]	0.540	0.108
δ	0–1	0.302[b]	0.375
F_0 (mm/day)	200–600	300.1	0.001
p_0 (mm/day)	0–10	7.45	0.320
a	0–1	0.0374	0.187
b	0–1	0.653	0.028
γ	0.2–5	2.03	0.296
G_0		0.48Gm	
q		0.38[b]	

[a] $0 \leq \alpha + \beta < 1$.
[b] multiply by 10^{-3}.

5.1. Test 1: Objective function for discharge

The value of χ^2 gives a quantitative measure of the model's ability to match the observations. Its value for each hydrological year is given in Table 3. Note that the value of χ^2 may not be reliable for years for which there is little flow at the gauge station for a large number of days (i.e. the 1990s).

As a further check we also compute the value of the relative error defined by

$$\varepsilon = \frac{\sum_i |Q_{0_i} - Q_{m_0}|}{\sum_i Q_{0_i}} \quad (29)$$

Note that the relative error will be dominated by the errors for low flow conditions, resulting in a potentially higher value for years with little or no total discharge through the gauging station. Also, the value of χ^2 is more sensitive than relative error to large errors at times of high flow rates.

For twenty four out of the twenty five years of record, the model's $\chi^2 < 1$. Most of the years (seventeen) have $\chi^2 < 0.1$, most of the remainder are low flow years. During the 1984–1985 wet season the model predicted a large flood event on days 140 and 141 (January 18 and 19) which was not recorded at the gauging station. The model predicts a flow of almost 100 cumecs on day 140 compared with the measured value of 11.2 cumecs. Despite intensive checks, the model predicted a higher discharge then what was recorded, in keeping with the large amount of rainfall that was actually recorded on day 140 (94 mm, over 12% of the annual rainfall for that year (749 mm), and almost 16% of the average annual rainfall). Note that a large amount of rainfall was recorded by all rainfall stations. If these two days are ignored, the χ^2 value drops 0.05. With the exception of the 1984 hydrological year, the highest χ^2 value occurs for 1991. This year is in the transition period where contribution to the surface discharge from *subf*2 is decreasing towards zero. The improvement in the model fit for 1994 indicates that the model, when calibrated on a period when both sub-surface flow mechanisms are in operation, is able to reproduce the hydrograph when only the fast flow component is contributing to the surface discharge. The model and measured daily discharge curves are shown in Fig. 5 for the hydrological years 1976 to 1981. The monthly discharge curves are shown in Fig. 6 for the entire period for which data is available.

The annual rainfall, runoff and runoff coefficient (runoff/rainfall) are shown in Fig. 7. There are two drought periods as clearly shown in the runoff coef-

Table 3
Values for the objective function $\chi 2$ and relative error ε for each hydrological year[a]

Year	χ^2	ε
1970–71	0.087	0.68
1971–72	0.027	0.52
1972–73	0.067	0.70
1973–74	0.020	0.71
1974–75	0.17	1.44
1975–76	0.39	1.08
1976–77	0.013	0.57
1977–78	0.34	0.51
1978–79	0.032	0.39
1979–80	0.094	0.44
1980–81	0.089	0.30
1981–82	0.025	0.22
1982–83	0.025	0.38
1983–84	0.025	0.25
1984–85	1.66	0.49
1985–86	0.032	0.53
1986–87	0.042	0.67
1987–88	0.077	0.61
1988–89	0.074	0.88
1989–90	0.033	0.96
1990–91	0.22	0.88
1991–92	0.97	1.14
1992–93	0.12	–
1993–94	0.11	0.69
1994–95	0.073	0.56

[a] Note that the high value of χ^2 for the 1984–85 hydrological year is reduced from 1.66 to 0.05 if the discharge for January 18 is set to the value predicted by the model (see text).

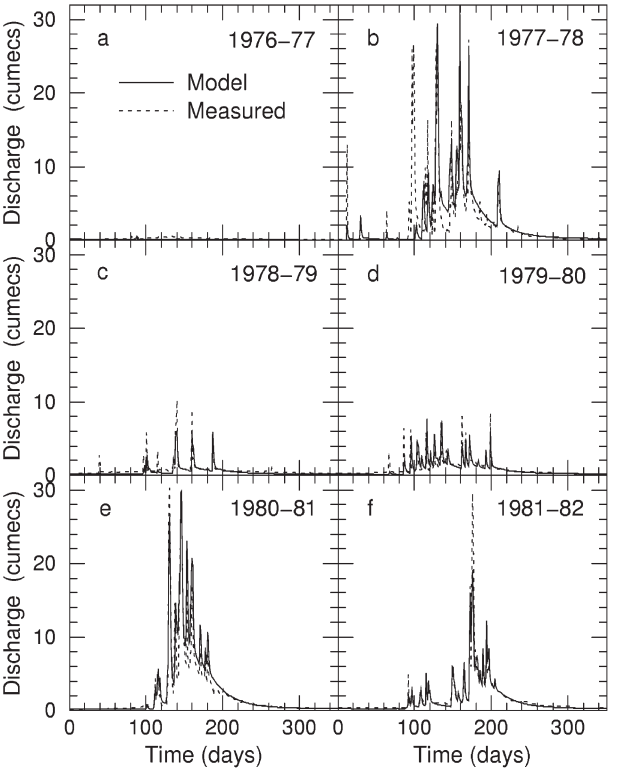

Fig. 5. Daily discharge at the catchment outlet at Phaistos for the 1977–78 to 1981–82 hydrological years.

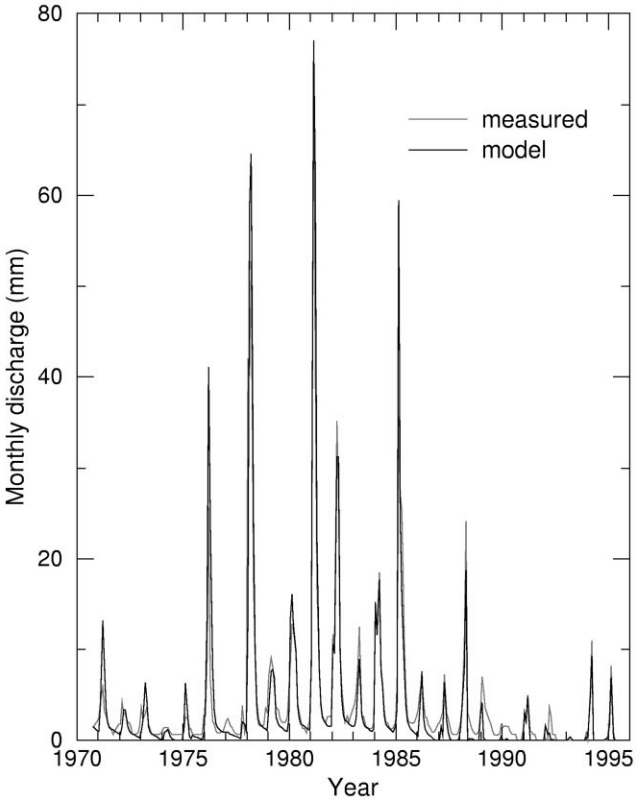

Fig. 6. Monthly discharge at the catchment outlet at Phaistos.

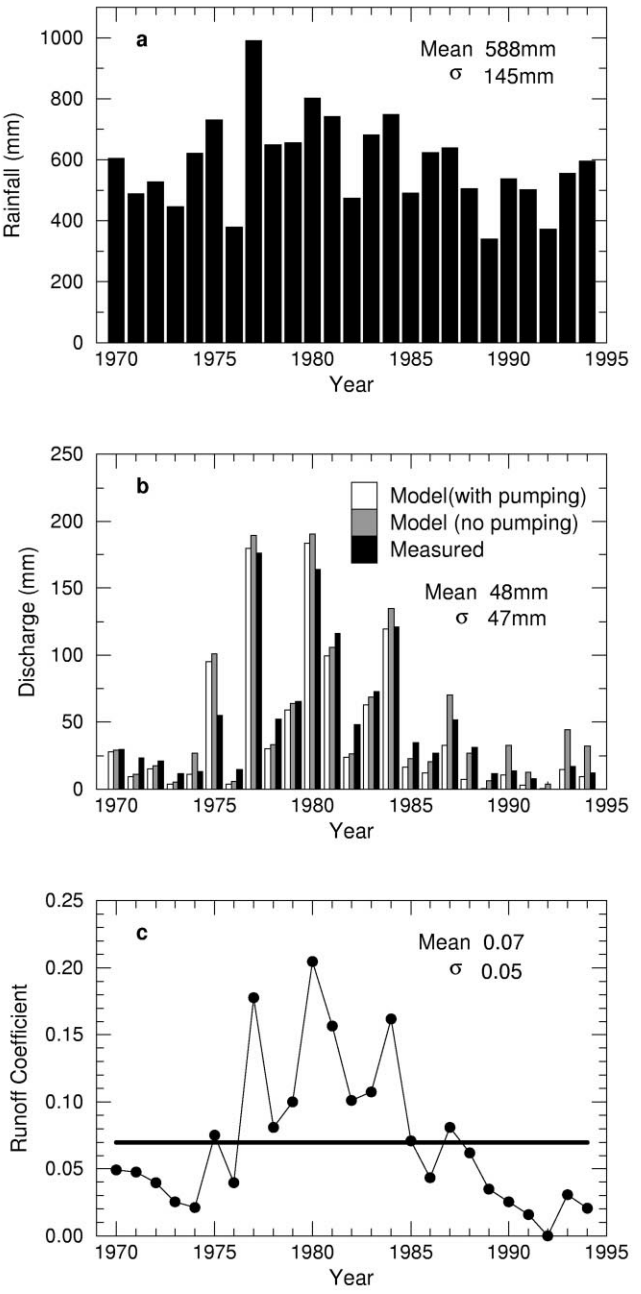

Fig. 7. Annual rainfall, discharge and runoff coefficient.

ficient. The 1970s fall in the runoff coefficient corresponds to a series of well below average rainfall years while in the 1990s the drop in the runoff coefficient reflects significant pumping of the groundwater store.

5.2. Test 2: Flow duration curve matching

As a further check of the performance of the model, a flow duration curve was created (Fig. 8) where the fraction of the days when the flow exceeded a particular flow rate is plotted against the flow rate. Starting with a selection of flow rates from 1 to 25 cumecs, the number of days for which the measured (and model) flow exceeded the chosen flow rate were determined. This was then converted to a percentage of the total number of days of data. The curve shows that the model is also reproducing well the frequency distribution of the measured discharge.

5.3. Test 3: Fourier analysis for the daily runoff coefficient

The rainfall (P) and runoff (Q) data were used to derive the daily runoff coefficient curve (r_c); which gives the fraction of a particular day's rainfall flows out of the catchment as a function of the number of days since the rain fell. Mathematically, this is the function which when convolved with the daily rainfall data produces the daily runoff data

$$Q = P \otimes r_c \tag{30}$$

To determine r_c, we use the Fourier transform of the above relation, giving

$$\mathcal{F}(Q) = \mathcal{F}(P) \times \mathcal{F}(r_c) \tag{31}$$

where $\mathcal{F}$ is the Fourier transform operator. Thus, r_c can be derived using

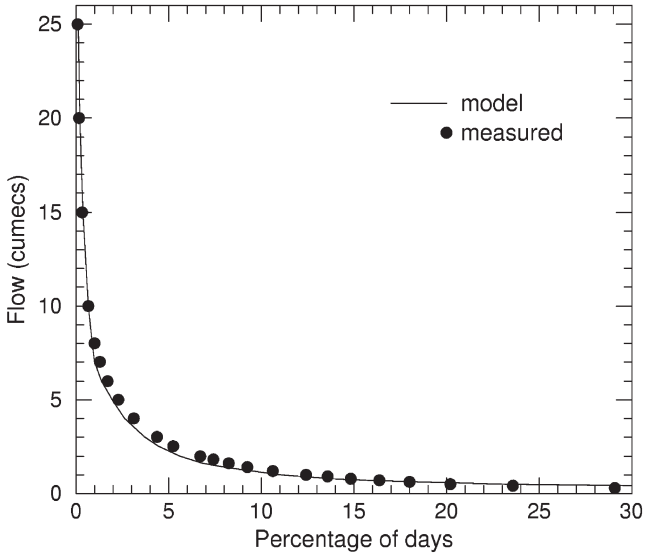

Fig. 8. Model and measured flow duration curves.

$$r_c = \mathcal{F}^{-1}\left(\frac{\mathcal{F}(Q)}{\mathcal{F}(P)}\right) \tag{32}$$

where $\mathcal{F}^{-1}$ is the inverse Fourier transform operator. This assumes that the only time-dependent quantities are the rainfall and discharge.

In a catchment such as the Messara Valley, which has large climate variations (dry summers, and wet winters), this assumption is not valid. The result will be increased noise in the runoff coefficients, limiting the period of high outflow just after rainfall. This can be seen in Fig. 9, where the daily rainfall coefficient is plotted for 9 days before and after rainfall. While there is considerable noise in the data prior to rainfall (indicating the typical standard deviation throughout the derived function is approximately σ =0.0016), the peak seen on the day of rainfall is more than 17σ, and the coefficients for the subsequent days decrease to 3.2σ on day 4. After this, the coefficients become lost in the noise. Despite this limitation, the analysis shows that for a typical rainy day, the effect of the rainfall is noticed at the flow station within 12 h (from the marked decrease in the runoff coefficient for the following day), and that, typically, almost 3% of the rainfall leaves the catchment within 12 h. In the first four days following the typical rainy day, a further 3% of the rainfall passes through the flow station. The value for the fast flow delay term, a=0.71, derived from Fig. 9 compares well with the value of 0.65 obtained from the model calibration.

5.4. Test 4: Qualitative groundwater level comparison

To compare fluctuations in the model groundwater storage (in mm of water) with measurements for a typical borehole in the Messara Plain aquifer, the model output must be converted from mm of water to depth of water level below the surface. In order to achieve this, we adopt an effective porosity profile with depth below the surface as shown in Fig. 10. Also shown are the specific yield estimates taken at various locations in the aquifer through pumping tests. Basically, we take a two

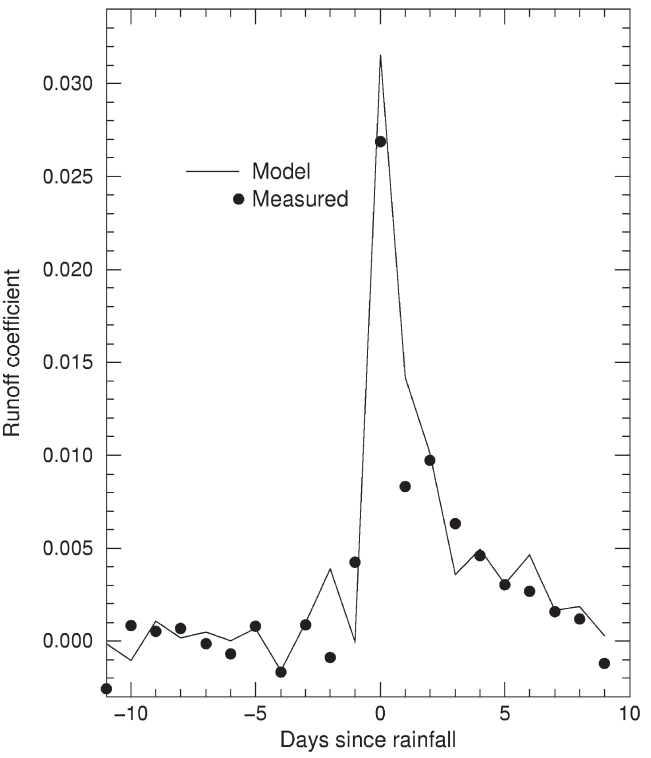

Fig. 9. Daily runoff coefficients derived from Fourier analysis of rainfall and discharge data (both measured and model). The non–zero values for days −11 to −1 (should be zero as these are days before rainfall) is due to the error introduced in assuming that only the rainfall and discharge are time dependent. The scatter in these values gives an estimate of the noise level throughout the curve.

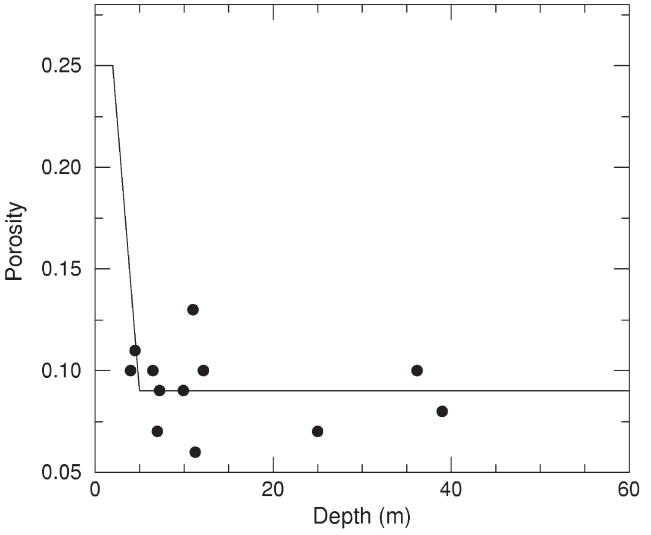

Fig. 10. Adopted model effective porosity with depth below surface, and measured specific yield for selected boreholes.

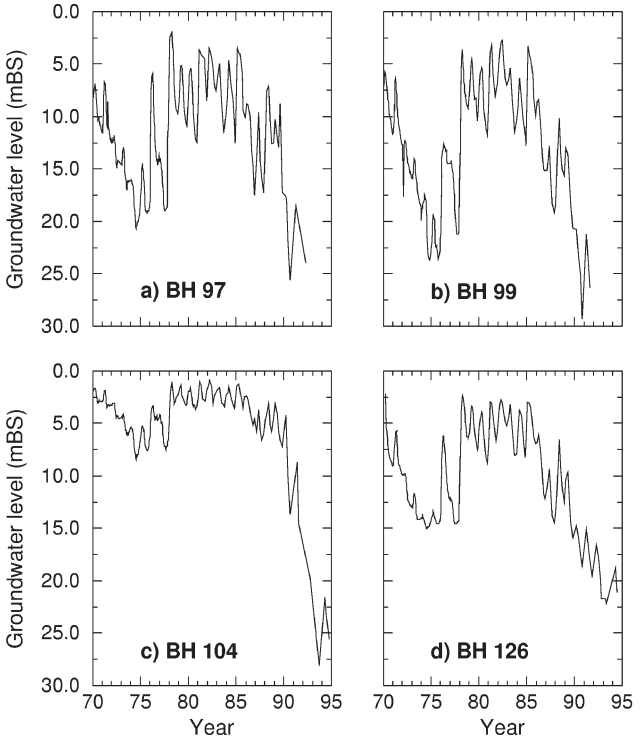

Fig. 11. Measured groundwater level in m above sea level (ASL) for bore holes on the Messara Plain.

layer model comprising a high porosity surface soil layer above the aquifer the area of the Messara Plain (112 km^2).

Examples of the measured groundwater level fluctuations at various boreholes along the river area are shown in Fig. 11. In Fig. 12a is shown the land-use development since the installation of the pumping network. It clearly shows the rapid rise in olive grove area under irrigation. The corresponding abstraction rate given in Fig. 12b was estimated from an application rate of 250 m^3/year per 1000 m^2 for olive groves, vines and cereals, and 600 m^3/year per 1000 m^2 for vegetables.

The model catchment mean groundwater storage with no groundwater natural loss and pumping set to the pre-network rate (7.5 Mm^3/year) for all years is shown in Fig. 13a. The model generates small groundwater fluctuations with essentially little inter-annual variation. If the natural loss from the groundwater store is now introduced then the fluctuations become more pronounced as shown in Fig. 13b. In Fig. 13c is shown the fluctuations for no natural loss but post-network pumping rate of 40 Mm^3/year, while Fig. 13d shows the fluctuations with natural loss and pumping rate as given in Fig. 12b for each year.

The estimated groundwater level fluctuations in metres below the surface (BS) are shown in Fig. 14. With natural loss and no irrigation pumping the model does not produce a significant drop in the observed groundwater level after 1984 (Fig. 14a), although it produces an early seventies drop in the groundwater level. The inclusion of the irrigation pumping results in interannual fluctuations (Fig. 14b) which reasonably follow the observed trends shown in Fig. 11.

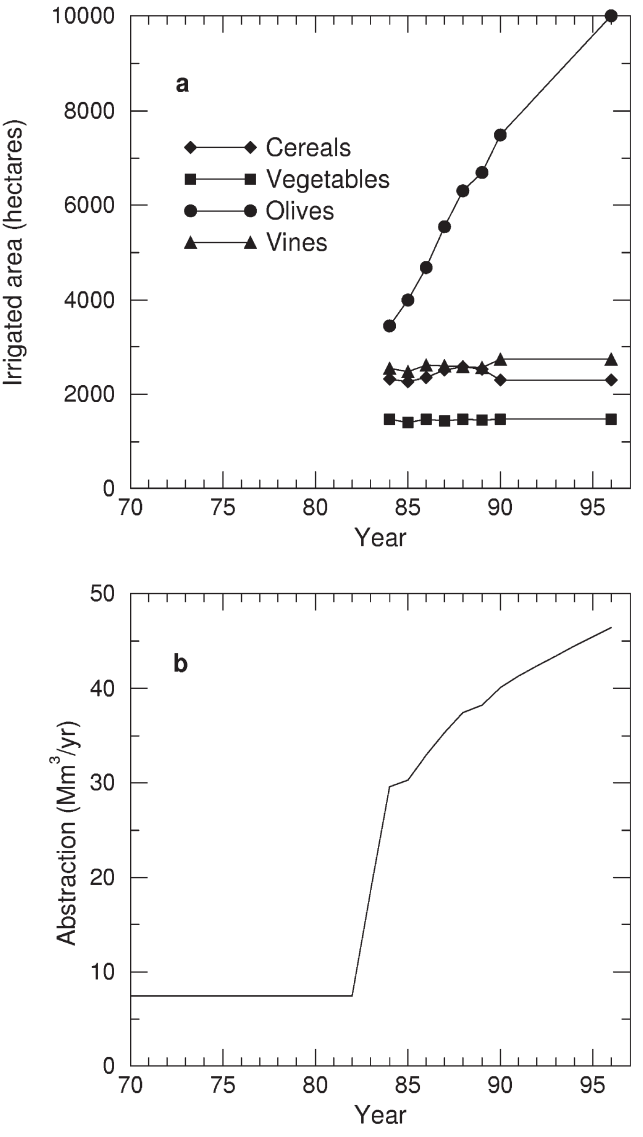

Fig. 12. Estimated groundwater abstraction and irrigated area.

6. Model predictions

6.1. Soil moisture and evaporation

The fluctuations in the model's soil moisture, evapotranspiration, and total natural evaporation loss (excluding irrigation) is shown in Fig. 15. The soil store fills up during the wet season and reaches, on average about 150 mm, whilst the actual evapotranspiration rate is around 1 mm/day in keeping with eddy correlation measurements (Vardavas et al., 1997). The total evaporation (evapotranspiration plus direct evaporation from

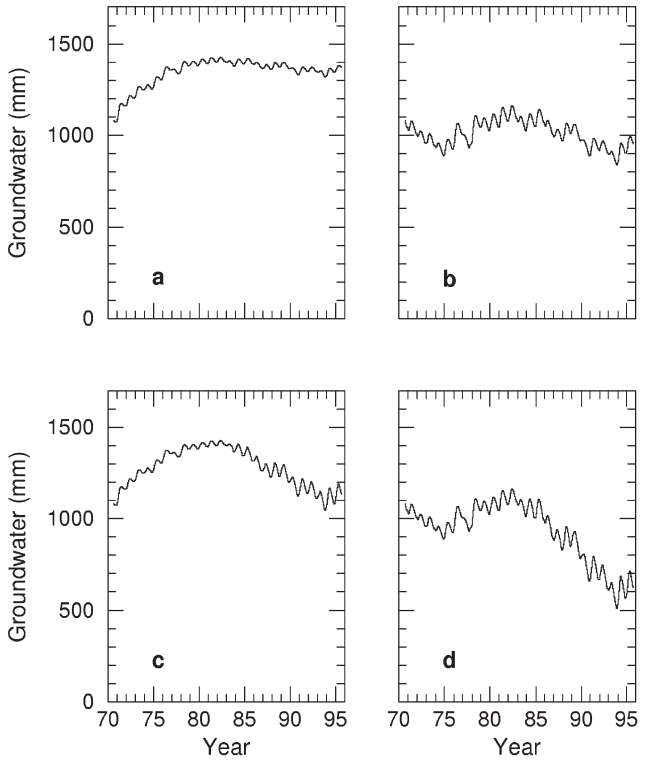

Fig. 13. Model mean groundwater storage in mm: (a) no natural loss and pre-network pumping; (b) with natural loss and pre-network pumping; (c) no natural loss and post-network pumping; (d) with natural loss and post-network pumping.

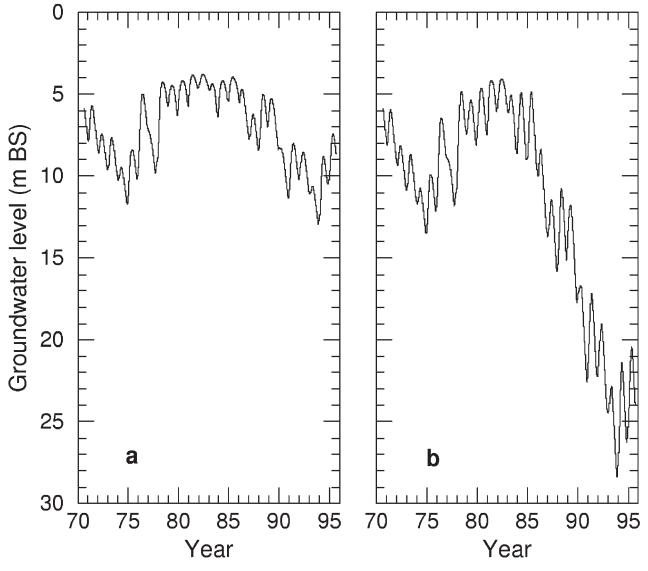

Fig. 14. Model mean groundwater level below surface (BS): (a) with natural loss and pre-network pumping rate; (b) with natural loss and post-network pumping.

the wet canopy and surface) peaks at 2 mm/day. The total actual natural evaporation has a minimum in summer which is determined by the surface expression of the groundwater. In Fig. 15 this minimum corresponds

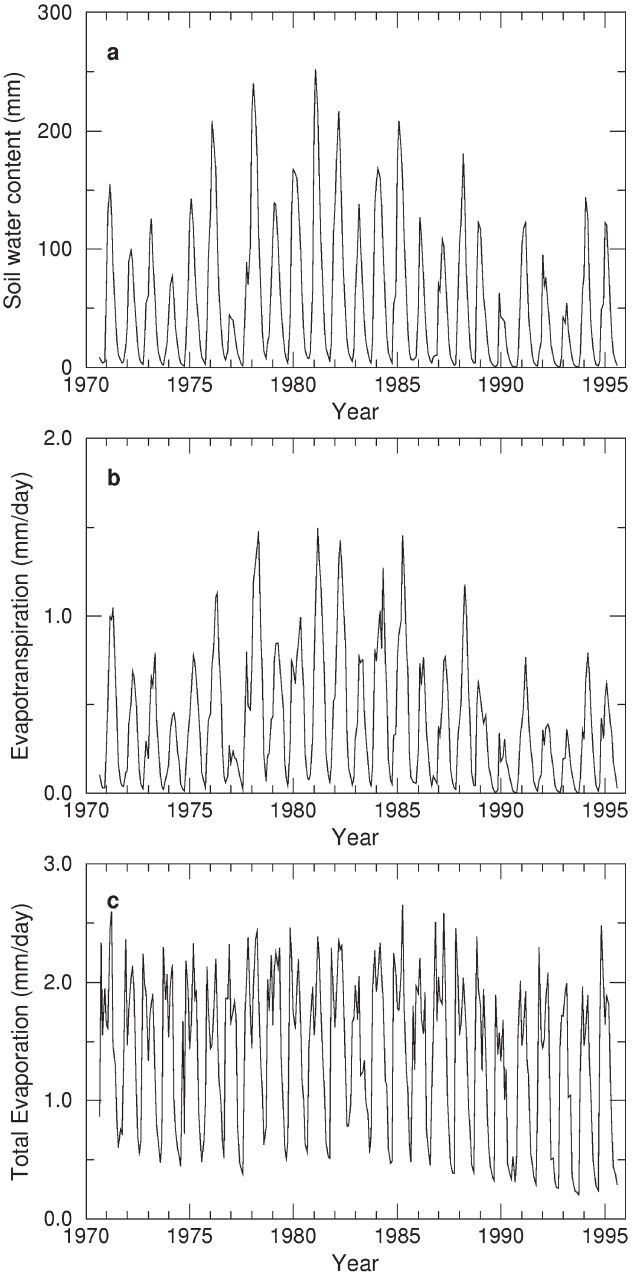

Fig. 15. Model soil water content, actual evapotranspiration and natural total evaporation (excluding irrigation, and assuming that groundwater natural loss is entirely in the form of evaporation of surface expressed groundwater).

to having all the groundwater natural loss going to evaporation. The trend in the minima has been towards zero as the groundwater storage has decreased significantly after 1985.

6.2. Recharge and pumping

Net recharge (R_n) of the groundwater store is determined from:

$$R_n = P - Q - E_{tot} - Q_{ss} \quad (33)$$

with P, Q and Q_{ss} representing rainfall, discharge and sub-surface outflow, respectively, and where total evaporation (E_{tot}) comprises evapotranspiration losses from the soil store, and evaporation from wet surfaces either through rainfall wetting or groundwater surface expression. In Fig. 16 is shown the net recharge on an annual basis together with the net recharge minus pumping. The variation clearly shows the negative net recharge over the early seventies which accounts for the declining groundwater levels over that period. This was followed by years of positive net recharge. Note the approximate 3–4 year cycle in the net recharge. It is interesting to note that some of the minima are close to El Nino drought years (1982, 1986, 1991). The effect of the pumping since 1984 has been to reduce the net recharge below zero. The associated drop in the groundwater level has reduced the runoff and the natural loss from the groundwater store.

6.3. Climate change and land-use scenarios

We have examined climatic change effects on groundwater levels due to possible future changes in rainfall for Crete based on a GCM scenario given by the UK Meteorological Office for the year 2050. We have not examined the enhanced evaporation that might arise due to large scale greenhouse effect warming of the region (e.g., Wigley, 1992), because of the uncertainties in estimating the actual regional surface radiation budget (e.g., Vardavas and Koutoulaki, 1995) under different climatic conditions. We have also examined land-use scenarios, that is, changes in irrigation pumping.

Fig. 17 shows the changes in the monthly rainfall predicted by the adopted GCM scenario for Crete. Generally, the prediction is for a significant reduction in early wet season rainfall. We have computed the actual monthly rainfall by applying the GCM predictions of percentage change in monthly rainfall to a monthly rainfall distribution for a typical year whose annual rainfall is close to the long-term mean of 588 mm. We have then used the daily rainfall pattern of this typical mean year and scaled it within each month by a constant factor so that the monthly total equals the predicted actual rainfall by 2050.

We then took as our starting point the hydrological year 1994–5 and applied different annual pumping rates for a typical mean year rainfall pattern and for a GCM scenario where the annual rainfall steadily decreases to reach the predicted 435 mm annual rainfall for the Messara Valley by 2050. The model was then run forwards in time to 2050 for each case. We have also examined the effect of different pumping scenarios adopting the past rainfall record of 25 years, starting with the rainfall

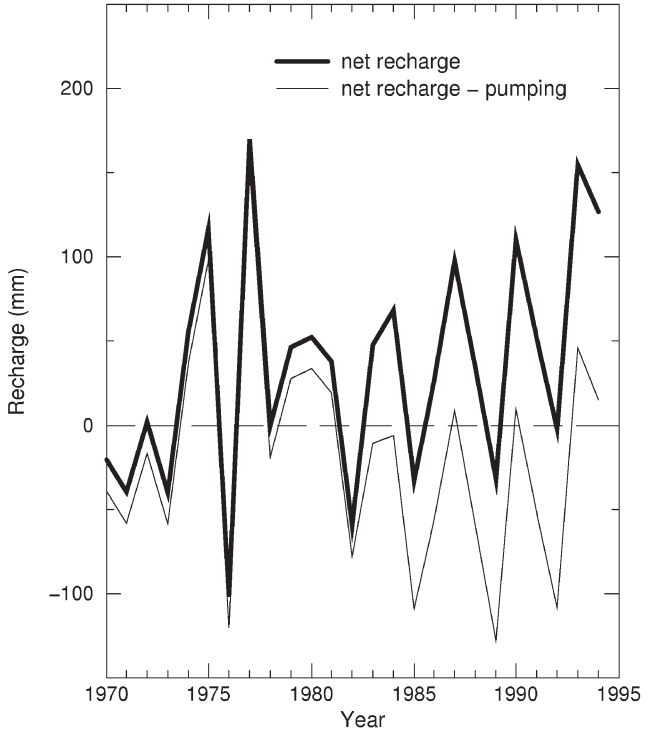

Fig. 16. Annual net recharge for the hydrological years from 1970 to 1994. Increase in net recharge in the 1990s is due to decreased surface runoff and groundwater loss from the catchment. Both discharge at the outlet and natural groundwater losses have decreased due to the increased agricultural pumping.

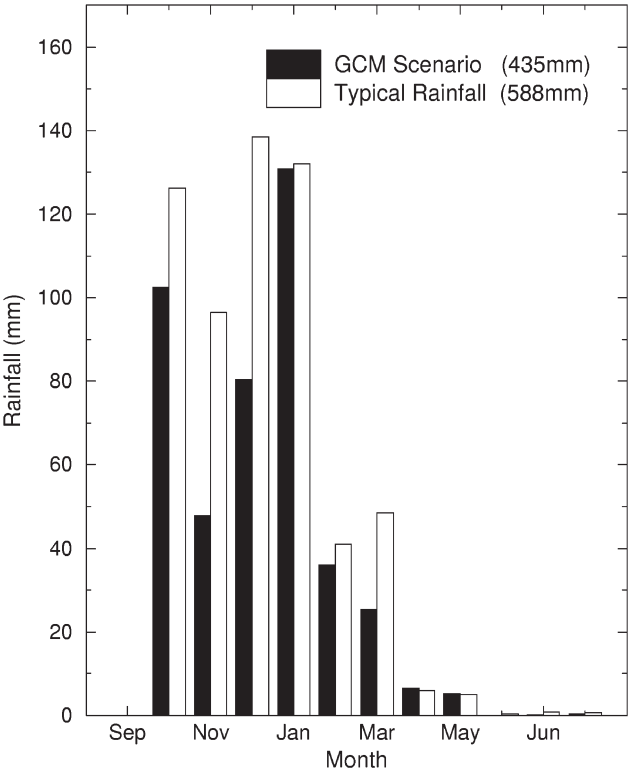

Fig. 17. Monthly rainfall pattern for a year with rainfall close to the mean (Typical Rainfall 588 mm) and GCM scenario modified monthly rainfall for a typical year rainfall pattern.

of the first year of record and running the programme forwards 25 years. Fig. 18 shows the groundwater level (m Below Surface) trends for three scenarios. Fig. 18a shows the groundwater level with time for different annual pumping rates assuming a typical mean year rainfall pattern for all future years. Fig. 18b shows the evolution of the groundwater level using the past rainfall record and Fig. 18c shows that for the GCM scenario. For the typical mean year rainfall pattern (Fig. 18a), equilibrium is reached after about 10 years. It would take about ten years for groundwater levels to rise by about 10 m if pumping is reduced to a pre-network pumping rate of 10 Mm^3/yr. For the estimated current annual rate of pumping (40 Mm^3), the groundwater level would rise a little while if the pumping rate were to increase to 60 Mm^3 then the groundwater level would fall further by 5 m, given average annual rainfall.

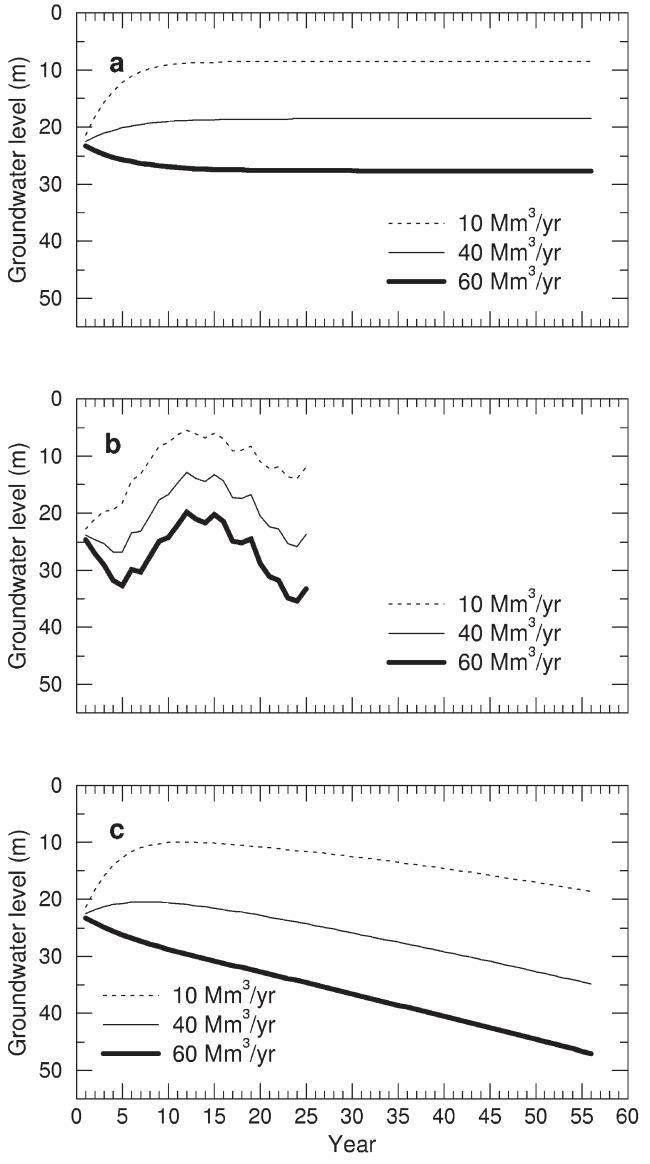

Fig. 18. (a) Model groundwater land-use scenario for typical mean year rainfall pattern for various pumping rates; (b) Model groundwater level variation using the 25 year rainfall record; (c) Model groundwater level trends for the GCM scenario of decreasing rainfall from 1995 to 2050.

Using the past rainfall record (Fig. 18b) the model demonstrates that it is possible for groundwater levels to rise during relatively wet years by about 10 m and fall an equal amount during relatively dry years.

The GCM scenarios for the groundwater level are more severe. If drier years do come then a return to a pre-network pumping rate would be required to maintain the groundwater level at its present level. The current pumping rate of about 40 Mm^3/yr may result in a further reduction in the groundwater level by 10 m by the year 2050. Any further increase in the annual pumping rate to 60 Mm^3 may result in the groundwater level falling by a further 20 m.

7. Conclusions

The original MAGELA rainfall-runoff model developed for the tropical wet-dry Magela Creek catchment in Australia has been modified and applied successfully to the Mediterranean wet-dry Messara Valley of Crete to take into account its steep topography. The model has also been used to model the discharge from the River Pang in the UK (GRAPES, 2000) indicating that the model can be applied to a wide range of climatic conditions.

The model was modified to include a two-component lateral sub-surface flow, one representing relatively fast flow to the catchment outlet (near-surface flow to channels on the Plain) and the other a slower flow (deeper flow from the surrounding mountains of the catchment). While the model was calibrated using data from September 1981 to August 1984 (a period when both components were contributing to the surface discharge), the model was still able to reproduce the measured discharge in the 1994 hydrological year (χ^2=0.073) when only the fast flow component remained. The model was also modified to give estimates of the recharge and fluctuations in the mean groundwater level. The model has been supplemented by two techniques for validation: derivation of the daily runoff coefficient through Fourier analysis of the measured rainfall and discharge; and comparison of model and measured flow duration curves.

The findings of this work are that climatic variability plays an important role in groundwater resource depletion along with irrigation pumping and natural loss of groundwater out of the Messara Valley. The average rainfall for the last 10 years of data (September 1985 to August 1995) was 516 mm/yr, a value below the long-term average of 588 mm/yr. The measured discharge at the catchment outlet at Phaistos was 21 mm/yr, which

compares well with the modelled discharge of 19 mm/yr. The direct actual evaporation plus evapotranspiration from the soil store amounted to an average of 336 mm/yr. Thus, the average annual recharge to the groundwater store was 159 mm/yr. For this period, the model gives an estimated loss of groundwater through evaporation and sub-surface outflow of 108 mm/yr, which coupled with an average abstraction rate of 97 mm/yr results in a net loss from the catchment's groundwater store of 46 mm/yr. Adopting the porosity profile for the Messara Plain aquifer given in Fig. 10, this implies an annual decrease in the groundwater level of approximately 1.5 m/yr, a value consistent with the observed 20 m drop over the last 10 years or so.

It is estimated that it would take at least 10 years for groundwater levels to rise to natural levels if the irrigation pumping rate were to be reduced to pre-irrigation network rates, under average rainfall conditions. The implications from a GCM scenario which predicts a future drier climate for Crete, due to climatic change, from a present long-term mean annual rainfall of 588 mm to 435 mm by 2050, is that groundwater levels might drop by a further 10 m. The fall in the groundwater level could be up to 20 m for any further increase in irrigation pumping. The model indicates that there might be a cycle in groundwater net recharge with near zero recharge every 3–4 years.

Acknowledgements

This research was supported by the European Union Environment and Climate Programme (contracts: EV5V-CT94-0466 and ENV4-CT95-0186). We would like to thank the local office of the Department of Agriculture for the hydrological data, especially Dimitris Papamastorakis. We would also like to thank the UK Meteorological Office and John Bromley of the Institute of Hydrology, Wallingford for the GCM scenario for Crete.

References

Brutsaert, W., 1984. Evaporation in the Atmosphere: Theory, History and Applications. D. Reidel, Dordrecht, The Netherlands, 299 pp.

Fantechi, R., Peter, D., Balabanis, P., Rubio, J.L., 1995. Desertification in a European context: Physical and socio-economic aspects, Final Report EUR 15415 EN 635pp., European Commission, Brussels.

FAO, 1972. Study of water resources and their exploitation for irrigation in eastern Crete. Overall study of the Messara Plain. AGL:SF/GRE 31, Tech Rep 1, 368 pp., United Nations Development Programme, Food and Agricultural Organization of the United Nations, Iraklion.

GRAPES, 1997. Groundwater and River Resources Action Programme on a European Scale: First Annual Report to the European Commission, ENV4 — CT95 — 0186, 134 pp.

GRAPES, 1998. Groundwater and River Resources Action Programme on a European Scale: Second Annual Report to the European Commission, ENV4 — CT95 — 0186, 200 pp.

GRAPES, 2000. GRAPES Technical Report, European Commission, ENV4 CT95-0186, 250 pp, March 2000.

Llamas, M.R., 1988. Conflicts between wetland conservation and groundwater exploitation: Two case histories in Spain. Environ. Geol. Water Sci. 11, 241–251.

Penman, H.L., 1948. Natural evaporation from open water, bare soil and grass. Proc. R. Soc. London Ser. A 193, 120–145.

de Rider, N.A., 1972. Study of water resources and their exploitation for irrigation in eastern Crete. Working document No. 26. Drilling and pumping tests in Messara. United Nations Development Programme, Food and Agricultural Organisation of the United Nations. Iraklion, AGC:SF/GRE 17/31.

Stringfield, V.T., LeGrand, H.E., 1971. Effects of Karst features on circulation of water in carbonate rocks in coastal areas. J. Hydrol. 14, 139–157.

UNCED, Earth Summit 92, 1992. The UN Conference on Environment and Development, Rio de Janeiro.

UNCED, 1994. United Nations Convention to Combat Desertification in those countries experiencing serious drought and/or desertification, particularly in Africa. New York, approved June 1994, Paris.

Vardavas, I.M., 1988. A simple water balance daily rainfall-runoff model with application to the tropical Magela Creek catchment. Ecol. Model. 42, 245–264.

Vardavas, I.M., 1989. A Fibonacci search technique for model parameter selection. Ecol. Model. 48, 65–81.

Vardavas, I.M., Koutoulaki, K., 1995. Model surface and top-of-atmosphere solar radiation budget for the Northern Hemisphere: Validation with ERBE satellite data. J. Geophys. Res. 100, 7303–7314.

Vardavas, I.M., Bolle, H.-J., Bromley, J., de Bruin, H., Devereux, B., Prastacos, P., 1996. An integrated monitoring and modelling study of desertification and climatic change impacts in the Messara Valley of Crete. EU DGXII, Environment and Climate Change Programme, Final Report EV5V-CT94-0466, 143 pp., November 1996.

Vardavas, I.M., Papamastorakis, J., Fountoulakis, A., Manousakis, M., 1997. Water resources in the desertification-threatened Messara Valley of Crete: estimation of potential evaporation. Ecol. Model. 102, 363–374.

Wigley, T.M.L., 1992. Future climate of the Mediterranean Basin with particular emphasis on changes in precipitation. In: Jeftic, L., Milliman, J.D., Sestini, G. (Eds.), Climate Change and the Mediterranean. Edward Arnold, London, p. 673.